

Two-scale method in the theory of scattering by fractal structures: One-dimensional regular problems

V. V. Konotop* and S. A. Bulgakov

*Institute for Radiophysics and Electronics, Academy of Sciences of the Ukraine,
Proscura Street 12, Kharkov 310085, The Ukraine, U.S.S.R.*

(Received 15 May 1991; revised manuscript received 4 November 1991)

In a recent paper one of the present authors [V. V. Konotop, *Phys. Rev. A* **44**, 1352 (1991)] put forth an analytical approach for the description of one-dimensional scattering by a Weierstrass-like layer. The method consists of splitting the fractal permittivity into two effective parts, the scales of which are long and short in comparison with a wavelength. The dependence of a splitting point on an incident wavelength is given. In the present paper we generalize such an approach, called a two-scale method (TSM) for a wide class of structures having irregularity, and provide complete analytical and numerical investigations of two particular cases: layers with Weierstrass-type and singular permittivities. A good correspondence between analytical predictions and numerical solutions of the corresponding Riccati equation, as well as qualitative agreement with outcomes published elsewhere [D. C. Jaggard and X. Sun, *IEEE Trans. AP-37*, 1511 (1989)], is observed. In all cases the scattering data have a strongly pronounced resonant character that is well described by the WKB approximation. Increasing the box dimension leads to growth of the internal scattering and, as a consequence, to the inapplicability of the TSM. To investigate the physical nature of this phenomena we study both the above problems in the Born approximation as well. The main feature of fractal layers consists of a noninteger-power-law dependence of scattering data on slab length. Application of the TSM allows one to find a number of harmonics (in the trigonometric-series expansion), enough to provide adequate numerical analysis of fractal layers. Validity limits of the theory developed are stated. They turn out to be approximately the same as those for the WKB approximation for the effective long-scale part of the fractal permittivity.

PACS number(s): 42.25.Fx, 61.10.Dp, 03.40.Kf

I. INTRODUCTION

Scattering by fractal media is an attractive subject for investigation for a number of reasons. It is stated that many natural objects (coastlines, clouds, the Earth's surface, systems of clusters, macromolecules, etc.) have a fractal structure (see, e.g., Refs. [1,2] for review). Nontrivial noninteger dimension stipulates an unconventional spectrum of the radiation scattered by such objects. Usually, fractals possess a wide range of scales, which makes traditional mathematical methods inapplicable in the region of small wavelengths. Namely, it is impossible to achieve the validity region of the Kirchhoff approximation for surface scattering and the WKB approximation for bulk scattering in the generally accepted sense [3]. This situation indicates a need for alternative mathematical methods. On the other hand, even the mathematical statement of the scattering problem requires a stipulation of the description by partial differential equations (say, Maxwell's equations) of a field reflected from an object having nondifferentiable geometry and appearance in connection with these "fractal" dispersion relations [4].

In spite of a series of recent publications, we do not as yet have an adequate mathematical theory for all the above questions. Moreover, some of the methods applied to such problems require verification of their validity.

To all appearances, the problem of the most popularity

now is scattering by fractal surfaces. It has been studied by Berry [3] and Berry and Blackwell [5], in the approximation of a small "topothesis," that is really equivalent to the Kirchhoff approach. Wong and Bray [6] examined the scattering by a solid-on-solid rough surface in the Born approximation. Scattering by fractal screens modulated surface fractal scattering has been investigated by Jakeman [7] and Jaggard and Kim [8]. The reflection of x-rays by fractal surfaces and porous solids was studied by Wong [9] and Sinha *et al.* [10].

A productive approach for fractal scattering has been reported by Jaggard and Kim [8] and Jaggard and Sun [11,12]. They developed the concept of band-limited fractals using the cutoff Weierstrass function as an example. Such an approach brings mathematical consideration nearer to natural phenomena, which always have a finite range of scales [13]. The dependence of diffractals, i.e., radiation scattered by fractal objects [3], on both fractal dimension [14] and number of tones was studied in detail. We note here only two results that will be useful to compare with our outcomes obtained below. In any case the increasing of D results in the same qualitative effects as increasing of roughness (for example, in the problem of scattering by fractal surfaces it leads to a rising of intensity of sidelobes [11]). The field scattered by a band-limited fractal fiber is insensitive to a number N of tones when $b^{(D-2)N} \ll 1 \ll b^N$ [12] [here b ($b > 1$) is a constant that is the same as γ in designations accepted in

the present work and given below by formula (2.3)].

Another approach for diffractals was developed by Mehaute and Heliodore [4]. They proposed a generalization of Maxwell’s equations for electromagnetism in fractal media. This generalization consists of the introduction of fractal (noninteger) derivatives. Although it allows one to understand some peculiarities of electromagnetic phenomena in fractal media, use of such an approach for scattering-data calculation is questionable.

Two one-dimensional diffractal problems were considered by Konotop, Yordanov, and Yurkevich [15] and Konotop [16]. In both papers the stationary problem was solved for the case of the “overbarrier” scattering by regular fractal slabs. In Ref. [15] wave transmission through a layer with a multifractal permittivity of the form of a Cantor-like object has been considered within the framework of a recursive relation for scattering data. This recursive relation was solved analytically in the Born approximation and numerically for arbitrary parameters. The main result of this work is that the transmission coefficient of the fractal slab has a set of transparency windows, the location points of which constitute a self-similar set. Also the method of a recursive relation is useful for comparison of different approaches. However, it has one essential restriction. The spatial structure of the permittivity must have a rather high symmetry for a recursive relation to be obtained.

To describe wave propagation through a slab with a permittivity described by a fractal function with a given spectrum, the two-scale method (TSM) has been proposed [16]. This method makes up the basis of the present work and allows one to derive an analytical expression for the scattering data for a number of cases. It is also to be pointed out that the TSM has a sense very close to the distorted-wave Born approximation developed by Sinha *et al.* [10] for surface scattering.

The organization of this paper is as follows. We start with the mathematical statement of the problem and description of different models of a fractal permittivity (Sec. II). Then in Sec. III we discuss peculiarities of the scattering by a fractal layer of small width (i.e., in the Born approximation). The principles of the two-scales approach in the general form are presented in Sec. IV. The next two sections (V and VI) are devoted to wave propagation through a Weierstrass-like slab and a layer having a singular permittivity, respectively. We carry out both analytical calculations within the framework of the TSM and numerical investigations of both problems. All results are summarized in the conclusion.

II. STATEMENT OF THE PROBLEM

In the present paper we consider the stationary one-dimensional Helmholtz equation

$$\frac{d^2\psi}{dx^2} + k^2[1 + \epsilon(x)]\psi = 0 \tag{2.1}$$

in which $\epsilon(x)$ is a fractal function restricted to the interval $[0, L]$:

$$\epsilon(x) = \begin{cases} \epsilon_0(x) & \text{at } 0 \leq x \leq L \\ 0 & \text{at } x < 0 \text{ and } x > L \end{cases} \tag{2.2}$$

It is more suitable for our purpose to use dimensionless variables. However, for convenience of interpretation we hold the traditional treatment as follows: k is a wave vector, $\epsilon_0(x)$ is a permittivity, and L is a layer width.

There are different definitions for fractal structures [1,2,13]. Each of them stresses some of the most important properties of these objects. In what follows we are interested in the algebraic property. This is a continuous but almost everywhere nondifferentiable function $\epsilon_0(x)$ that is understood as a “fractal.” Historically the Weierstrass function

$$\epsilon_0(x) = \epsilon_w(x) = \epsilon_0(1 - \gamma^{D-2}) \sum_{n=0}^{\infty} \frac{\cos(\gamma^n x)}{\gamma^{(2-D)n}} \tag{2.3}$$

is the most popular specimen of such a class of functions. In this definition D is in the range $1 < D < 2$ and plays the part of the box dimension of $\epsilon_0(x)$ [17]; γ is a scaling parameter, it must be greater than unity ($\gamma > 1$); the constant ϵ_0 has the meaning of an amplitude of permittivity variations, and factor $(1 - \gamma^{D-2})$ is introduced to make the absolute value of $\epsilon_0(x)$ be not more than ϵ_0 .

From the mathematical point of view the Weierstrass function is an absolutely summable trigonometric set of an everywhere nondifferentiable function (see, e.g., Ref. [18]). It satisfies the Lipschitz continuity condition with the exponent $2 - D$. While considering physical systems one deals with differentiable functions (that may be rapidly oscillating) rather than with mathematical fractals. Usually the spectrum decay is considered as the main characteristic. In this sense some properties of a fractal medium can be simulated by a function the derivative of which may exist but which is not homogeneously restricted. In this context we also investigate another kind of permittivity given by the trigonometric series

$$\epsilon_0(x) = \epsilon_\alpha(x) = \epsilon_0 \sum_{n=1}^{\infty} \frac{\cos(nx)}{n^\alpha}, \tag{2.4}$$

with $0 < \alpha < 1$. This function is divergent at $x \rightarrow 0$. Namely, there is an asymptotic [18]

$$\epsilon_\alpha(x) \sim \epsilon_0 x^{\alpha-1} \Gamma(1-\alpha) \sin \frac{\pi\alpha}{2} \text{ at } x \rightarrow 0 \tag{2.5}$$

where $\Gamma(x)$ is a gamma function. That is why for the sake of definiteness we call ϵ_α a “singular permittivity.” Also, since function $\epsilon_\alpha(x)$ is periodic it must be considered for $L \in [0, 2\pi)$ only.

In what follows we concentrate our attention on the permittivities of both types: (2.3) and (2.4). The main subject of our investigation will be the scattering data, i.e., the reflection (r_L) and transmission (t_L) coefficients of a corresponding slab. Since we are interesting in the layer characteristics it will be suitable to make use of the following representation (see, e.g., [19]):

$$T_L = |t_L|^2 = \frac{4}{k^2 S^2(L) + S'^2(L) + C^2(L) + k^{-2} C'^2(L) + 2} \tag{2.6}$$

where $S(x)$ and $C(x)$ are solutions of Eq. (2.1) with the boundary conditions $C(0)=S'(0)=1$ and $S(0)=C'(0)=0$; the prime means the derivative with respect to the argument.

As is well known, the reflection coefficient can be examined within the framework of the Riccati equation [$r_L=r(x=L)$]:

$$\frac{dr(x)}{dx} = 2ikr(x) + \frac{ik}{2}\epsilon_0(x)[1+r(x)]^2. \quad (2.7)$$

The initial condition for this equation is

$$r(x=0)=0. \quad (2.8)$$

To conclude this section we note that both the above types of permittivity belong to a wide class of functions, which are represented in a form of the trigonometric series

$$\epsilon_0(x) = \sum_{n=0}^{\infty} a_n \cos(k_n x + \phi_n), \quad (2.9)$$

where a_n is an amplitude of a harmonic with the wave number k_n and phase ϕ_n . It is believed that nondifferentiable (fractal) functions can be obtained from Eq. (2.9), with nonzero phase and particular relations

$$a_n = a(k_n) \sim k_n^{-\alpha}, \quad k_n \sim n, \quad 0 < \alpha < 1 \quad \text{at } n \rightarrow \infty. \quad (2.10)$$

The presence of phases ϕ_n in Eq. (2.9) allows one also to simulate various random functions with the help of such a representation [8,17].

$$r_L = -\frac{k}{2} e^{2ikL} \epsilon_0 (1 - \gamma^{D-2}) \sum_{n=0}^{\infty} \frac{1}{\gamma^{(2-D)n} (4k^2 - \gamma^{2n})} \times [-2k + 2ke^{-2ikL} \cos(\gamma^n L) + i\gamma^n e^{-2ikL} \sin(\gamma^n L)]. \quad (3.2)$$

The behavior of the reflection coefficient of a thin slab (i.e., its dependence on the slab width) in the limiting case

$$\epsilon_0 kL \ll 1 \quad (3.3)$$

is described by the formula (it is evaluated in Appendix A):

$$r_L = \frac{ikL}{2} \epsilon_0 + \rho_0 (\epsilon_0 kL)^{3-D}. \quad (3.4)$$

Here

$$\rho_0 = \frac{i(\epsilon_0 k_0)^{D-2}}{2(D-4 \ln \gamma)} \sum_{n=-\infty}^{\infty} p_{0n} \Gamma(p_{0n}) \cos \left[\frac{\pi p_{0n}}{2} \right] \exp \left[-\frac{2\pi i n}{\ln \gamma} \ln L \right]$$

and

$$p_{0n} = \frac{2\pi i n}{\ln \gamma} - 4 + D.$$

The item with the noninteger power of L in the Born expansion (3.4) manifests a diffractal nature. The scattering now is much stronger than the scattering by usual (nonfractal) objects having the same length. In the latter case the second term of the expansion is of $(\epsilon_0 kL^2)$ order and hence, taking inequality (3.3) into account, is much less than that in Eq. (3.4) (if ρ_0 of course is not abnormally large). The intensity of the backscattering grows with an

III. BORN APPROXIMATION

As was pointed out in Ref. [16], even in the Born approximation one can observe some peculiarities of scattering by fractal structures. In order to state the physical nature of such peculiarities we consider now the solution of the Riccati equation (2.7) under the assumption that the absolute value of the reflection coefficient is small enough: $|r_L| \ll 1$. Neglecting r_L in comparison with unity in the right-hand side of Eq. (2.7) we get a simple linear equation. Its solution is

$$r_L = \frac{ik}{2} e^{2ikL} \int_0^L \epsilon_0(x) e^{-2ikx} dx. \quad (3.1)$$

Thus, roughly speaking the reflection coefficient is determined by the area under the fractal curve, i.e., area of a polygon with a fractal boundary. This value must be connected with the box dimension of the curve $\epsilon_0(x)$ (see, e.g., Ref. [2]). This means, in particular, that the expansion of the reflection coefficient absolute value in terms of small L may contain fractional powers.

Let us consider two examples.

A. Weierstrass-type permittivity

Inserting the permittivity in the form of the Weierstrass function (2.3) into Eq. (3.1) and integrating each term one can easily obtain

increasing of the fractal dimension (cf. with the results by Jaggard and Sun [11] mentioned in the Introduction). The obtained result also means that a wave "feels" really a small-scale structure and, hence, that a diffractal possesses the information about the box dimension of the object irradiated.

B. Singular permittivity

Now we consider an example indicating more strongly irregular properties. Inserting the asymptotic (2.5) for $\epsilon_\alpha(x)$ directly into Eq. (3.1) we get the reflection

coefficient of a slab with the singular permittivity

$$r_L = \epsilon_0 \frac{ik\pi}{4 \cos(\pi\alpha/2)} e^{2ikL} L^\alpha \gamma^*(\alpha, 2ikL). \quad (3.5)$$

Here

$$\gamma^*(\alpha, 2ikL) = \frac{(2ik\pi)^{-\alpha}}{\Gamma(\alpha)} \gamma(\alpha, 2ikL).$$

$\gamma(\alpha, 2ikL)$ is an incomplete gamma function. Using the expansion of $\gamma^*(\alpha, 2ikL)$ into the power series [20] under the preliminary assumption (3.3) one can represent r_L in a form

$$r_L = \frac{ik\pi}{4 \cos(\pi\alpha/2)} \epsilon_0 L^\alpha \sum_{n=0}^{\infty} \frac{(2ikL)^n}{\Gamma(\alpha+n+1)} \quad (3.6)$$

and consequently in the limit $L \rightarrow 0$

$$r_L = \rho_\alpha \epsilon_0 k L^\alpha, \quad (3.7)$$

where $\rho_\alpha = i\pi/[4 \cos(\pi\alpha/2)\Gamma(\alpha+1)]$. Thus, due to the singular structure one can observe an anomalous scattering. It is interesting to note that in the case $\alpha = \frac{1}{2}$ the power dependence of $R_0 = |r_L|^2$ on L coincides with that obtained for the reflection coefficient of a thin layer with a Gaussian δ -function-correlated random permittivity: $R_0 \sim L$.

Returning to the restriction $R_0 \ll 1$ with r_L defined by (3.7) we come to the limiting inequality

$$\rho_\alpha \epsilon_0 k L^\alpha \ll 1. \quad (3.8)$$

Taking into account that the production $\rho_\alpha \epsilon_0$ now plays the part of an amplitude the comparison of (3.8) with Eq. (3.3) (remember $\alpha < 1$) leads to the conclusion that the Born approximation in the case of the singular fractal permittivity may fail at more short distances than in the case of any well-differentiable function.

IV. TWO-SCALE APPROACH

In the preceding section we have considered the range of sufficiently large wavelengths. Conventionally, the opposite limit is called the quasiclassical or WKB approximation. The main requirement of such an approach is the smallness of a wavelength in comparison with the scale of permittivity variations (see, e.g., Refs. [21,22]). The estimation of the corresponding relation may be given with the help of the derivation of $\epsilon_0(x)$ with respect to the argument. Since such a derivative does not exist for the fractal functions under consideration, it is evident that the quasiclassical approximation in the usual sense is not applicable for the description of waves in such media. The physical reason for this feature is the fact that fractal structures possess all scales, including scales being less than any wavelength.

At the same time, in the theory of surface scattering the so-called two-scale method [10,23,24] is applied satisfactorily for a number of situations. It is based on the possibility under definite physical conditions to split the spectrum of the scattering object (say, of a surface form) into two parts, one of which corresponds to the slow variations in comparison with the wavelength, and another

one describing small scale fluctuations. Such splitting allows a use of different approaches for the description of the different parts.

Recently one of the authors [16] has proposed application of an analogous method for the description of scattering by regular fractal layers. Now we describe this method in a general form for the permittivity (2.9).

A. Transmission coefficient

Let the spectrum of the fractal permittivity contain wave numbers being greater than K^* (where K^* is a constant). Let also an incident wave number k be much greater than K^* ($k \gg K^*$), which means that the wavelength belongs to an internal part of a scale range. Finally, let one find such a number H depending on k for which the two following requirements will be satisfied.

(i) The set

$$\Delta\epsilon_N(x) = \sum_{n=N}^{\infty} a_n \cos(k_n x + \phi_n) \quad (4.1)$$

in the definite sense is much less than the sum $1 + \epsilon_N(x)$

$$\epsilon_N(x) = \sum_{n=0}^{N-1} a_n \cos(k_n x + \phi_n), \quad (4.2)$$

say, for example,

$$\int_0^L dx |\Delta\epsilon_N(x)| \ll \int_0^L dx |\epsilon_N(x) + 1| \quad (4.3)$$

[the exact requirement can be stated at the end of calculations and the inequality (4.3) is considered now as the previous necessary condition].

(ii) The function $\epsilon_N(x)$ is slowly varying on the scale of the wavelength:

$$\left| \frac{d\epsilon_N(x)}{dx} \right| \ll k |1 + \epsilon_N(x)|. \quad (4.4)$$

Then one can employ the following expansion for the field ψ :

$$\psi = \psi_0 + \psi_1 + \dots \quad (4.5)$$

($|\psi_0| \gg |\psi_1| \gg \dots$) where ψ_0 is a solution of the Helmholtz equation with the permittivity $\epsilon_N(x)$:

$$\frac{d^2\psi_0}{dx^2} + k^2[1 + \epsilon_N(x)]\psi_0 = 0. \quad (4.6)$$

Due to the requirement (4.4) the last equation can be solved in the WKB approximation. Two independent solutions are obtained immediately

$$S_k(x) = \frac{\sin[kS(0,x)]}{kq_N^{1/4}(0)q_N^{1/4}(x)}, \quad (4.7a)$$

$$C_k(x) = \frac{\cos[kS(0,x)]}{q_N^{1/4}(x)} q_N^{1/4}(0), \quad (4.7b)$$

where

$$S(y,x) = \int_y^x q_N^{1/2}(z) dz, \quad (4.8)$$

$$q_N(x) = 1 + \epsilon_N(x). \quad (4.9)$$

In accordance with (2.6) the functions (4.7) form the main value of the transmission coefficient.

The fractal part $\Delta\epsilon_N(x)$ of the permittivity can be taken into account in the next order. The function ψ_1 solves the equation

$$\frac{d^2\psi_1}{dx^2} + k^2[1 + \epsilon_N(x)]\psi_1 = -k^2\Delta\epsilon_N(x)\psi_0. \quad (4.10)$$

First replacing $\psi_0(x)$ by $S_k(x)$ and then by $C_k(x)$, one can obtain to first order two independent normalized solutions

$$S(x) = S_k(x) + I_S(x)/q_N^{1/4}(x)q_N^{1/4}(0), \quad (4.11a)$$

$$C(x) = C_k(x) + I_C(x)q_N^{1/4}(0)k/q_N^{1/4}(x). \quad (4.11b)$$

Here

$$I_S(x) = \frac{1}{2} \int_0^x dx' \frac{\Delta\epsilon_N(x')}{q_N^{1/2}(x')} (\cos[kS(0,x)] - \cos\{k[S(0,x') + S(x,x')]\}), \quad (4.12a)$$

$$I_C(x) = \frac{1}{2} \int_0^x dx' \frac{\Delta\epsilon_N(x')}{q_N^{1/2}(x')} (\sin\{k[S(0,x') + S(x,x')]\} + \sin[kS(0,x)]). \quad (4.12b)$$

Finally, the insertion of Eqs. (4.11) into the expression for T_L (2.6) gives with the accuracy accepted

$$T_L = T_0 - \frac{kT_0^2}{2\sqrt{q_N(0)q_N(L)}} \times \{I_S(L)\sin[kS(0,L)][1 - q_N(0)q_N(L)] + I_C(L)\cos[kS(0,L)][q_N(0) - q_N(L)]\}. \quad (4.13)$$

Here

$$T_0 \equiv T_0(L) = \frac{4\sqrt{q_N(0)q_N(L)}}{[1 + \sqrt{q_N(0)q_N(L)}]^2 - [1 - q_N(0)][1 - q_N(L)]\cos^2[kS(0,L)]} \quad (4.14)$$

is an expression for the transmission coefficient in the WKB approximation.

It should be noted that Eq. (4.13) gives the trivial result $T_L = 1$ if $\epsilon_N(x) \equiv 0$. In order to provide the transition to the Born approximation it is necessary to expand the solution (4.14) and general representation (2.6) up to the second order in $\Delta\epsilon_N(x)$.

B. Discussion

Equation (4.13) is fundamental for the TSM. The first term T_0 corresponds to the boundary scattering, since as known from the WKB theory the scattering by large scales is exponentially small. That is why T_0 essentially depends on the boundary points 0 and L [see Eq. (4.14)]. It also means that this term describes so-called resonance effects well known in quantum mechanics [25]. The peculiarity of the case under consideration lies in the fact that the second boundary “level” depends on the layer width L . Thus, in addition to the resonance oscillations one can observe essential variations of their amplitude with the distance L .

The second term contains integrals over the slab length and depends on the fractal addendum $\Delta\epsilon_N(x)$. It describes the small scale (or fractal) scattering.

At the same time neither formula (4.13) nor (4.14) gives a final answer, since we do not have yet a relation between the “dividing” number N and the wave vector k . Intuitively it is clear that larger H corresponds to larger k and that N must be determined from the relation bounding k with a wave number of one of the permittivity expansion harmonics.

From the mathematical viewpoint the choice of N has

to coordinate the requirements (4.3) and (4.4). It gives an upper bound for N [the derivative of $\epsilon_N(x)$ with respect to the argument grows with N]. The requirement (4.3) provides the lower limit, which, generally speaking, is related to the slab width. As is clear, increasing the splitting point leads to an increase in the largest width for which the TSM is still valid (since the fractal part of the scattering data grows with L and decreases with N). Also the choice must forbid both exceeding the acceptable accuracy and changing the expansion order (the last condition means that the first term of the direct expansion must be much greater than the next WKB term, not represented here). All these reasons allow one to make the following statement: the dividing number N depends on the wave number k and must be found from the relation

$$k_N = k, \quad (4.15)$$

where k_N is a wave number of the N th harmonic in the permittivity expansion. It means, in particular, that the method is applicable when the wavelength is much less than the largest scale of the permittivity variation. Its leading order corresponds in that case to the conventional WKB approximation.

It is noteworthy that Eq. (4.15) is written with some accuracy, which provides k belonging to the interval determined by (4.3) and (4.6) (a typical situation in the two-scale approach [24]).

By formulas (4.13)–(4.15) we have solved the problem under consideration. The leading term T_0 of the transmission coefficient can be represented now in a “more physical” form:

$$T_0(L) = \frac{4\sqrt{q_k(0)q_k(L)}}{[1 + \sqrt{q_k(0)q_k(L)}]^2 - \epsilon_k(0)\epsilon_k(L)\cos^2[kS(0,L)]} \tag{4.16}$$

Here for $q_k(x)$ and $\epsilon_k(x)$ one has to hold only harmonics having scales greater than the wavelength.

Let us consider the first-order term in more detail. To this end taking into account the presentation (2.9) we rewrite functions $I_{S,C}(L)$ defined by (4.12) in the following way:

$$I_{\{S\}}(L) = \frac{1}{2} \sum_{n=N}^{\infty} a_n [I_{\{S\}}^{(+)}(L;n) + I_{\{S\}}^{(-)}(L;n) + I_{\{S\}}^{(1)}(L;n)] \tag{4.17}$$

where

$$I_{\{S\}}^{(+)}(L;n) = \frac{1}{2} \int_0^L \frac{dx}{q_N^{1/2}(x)} \left\{ \begin{matrix} \sin \\ -\cos \end{matrix} \right\} f_+(x,n) \tag{4.18}$$

$$I_{\{S\}}^{(-)}(L;n) = -\frac{1}{2} \int_0^L \frac{dx}{q_N^{1/2}(x)} \left\{ \begin{matrix} \sin \\ \cos \end{matrix} \right\} f_-(x,n) \tag{4.19}$$

$$I_{\{S\}}^{(1)}(L;n) = \left\{ \begin{matrix} \sin \\ \cos \end{matrix} \right\} [kS(0,L)] \int_0^L \frac{dx}{q_N^{1/2}(x)} \cos(k_n x + \phi_n) \tag{4.20}$$

and

$$f_{\pm}(x,n) = k_n x \pm kS(0,x) \pm kS(L,x) + \phi_n$$

Since we are seeking the solution in the region of the large wave numbers [i.e., when the condition (4.4) is valid] the function $q_N(x')$ in the integrands in Eqs. (4.18)–(4.20) can be regarded as a slowly varying one. It allows one to apply the stationary-phase method to evaluate $I_{\{C/S\}}(L)$. Differentiation of the functions $f_{\pm}(x,n)$ yields that only the integral (4.19) has stationary-phase points $x_m(n)$ (there $m = 1, 2, \dots, M$, M is a number of such points and it is designated that x_m depends on a harmonic number n) which satisfy the equation

$$\epsilon_N(x_m(n)) = \frac{k_n^2}{4k^2} - 1, \quad \left[q^{1/2}(x_m(n)) = \frac{k_n}{2k} \right] \tag{4.21}$$

Thus, if Eq. (4.21) has a solution, to the leading order the sum (4.17) can be reduced to

$$I_{\{S\}}(L) = -\sqrt{k\pi} \sum_{n=N}^{\infty} \sum_{m=1}^M \frac{a_n}{k_n} \left| \frac{d\epsilon_N(x_m)}{dx_m} \right|^{-1/2} \times \left\{ \begin{matrix} \sin \\ \cos \end{matrix} \right\} \left[f_-(x_m;n) + \frac{\pi}{4} \delta_m \right] \tag{4.22}$$

where

$$\delta_m = \text{sgn} \left[-\frac{d\epsilon_N(x_m)}{dx_m} \right] \tag{4.23}$$

and one has to keep in mind that the number of stationary-phase points depends on n [$M \equiv M(n)$] so that generally speaking one cannot change the summation order.

The total dependence of M on the tone number results only from the condition (4.22). It follows, in particular, that the number of stationary-phase points decreases with growth of n , and the external sum in Eq. (4.21) is restricted by a number N^* which is determined by the relation

$$(k_N^*)^2 = 4k^2(1 + \epsilon_{\max}) \tag{4.24}$$

if $\epsilon_{\max} = \max[\epsilon(x)]$ exists. Then, taking into account general relation (2.10) $a_n \sim k_n^{-\alpha}$ (at $n \geq N \gg 1$), one can modify (4.22) to

$$I_{\{S\}}(L) = -\sqrt{k\pi} \sum_{n=N}^{N^*} \sum_{m=1}^M k_n^{-(1+\alpha)} \left| \frac{d\epsilon_N(x_m)}{dx_m} \right|^{-1/2} \times \left\{ \begin{matrix} \sin \\ \cos \end{matrix} \right\} \left[f_-(x_m;n) + \frac{\pi}{4} \delta_m \right] \tag{4.25}$$

Exact calculation of this expression by analytical methods only seems to us to be impossible. However, an estimate of its upper bound is enough for our goals. Correspondingly we write

$$\left| I_{\{S\}}(L) \right| \leq I^* = \sqrt{k\pi} \sum_{n=N}^{N^*} k_n^{-(1+\alpha)} \sum_{m=1}^M \left| \frac{d\epsilon_N(x_m)}{dx_m} \right|^{-1/2} \tag{4.26}$$

Let ϵ' and ϵ be any characteristic values of $d\epsilon_N(x)/dx$ and $\epsilon_N(x)$ be on the interval $(0,L)$. Then the number of stationary-phase points can be estimated as $M \sim L\epsilon'/\epsilon$. Thus we have

$$I^* \sim \sqrt{k\pi} L \frac{\sqrt{\epsilon'}}{\epsilon} \sum_{n=N}^{N^*} k_n^{-(1+\alpha)} \tag{4.27}$$

Taking into account that

$$\sum_{n=N}^{N^*} \frac{k}{k_n^{1+\alpha}} \leq \text{const} \times a_N (1 + \epsilon_{\max}) \tag{4.28}$$

which follows from the definition (4.24), and combining this with (4.4), (4.12), and (4.27), we finally conclude

$$I^* \ll A(1 + \epsilon_{\max}) a_N L$$

where A is a constant of order unity. Consequently the fractal part of the transmission coefficient can be neglected in the leading order if

$$A(1 + \epsilon_{\max}) a_N kL \leq 1 \tag{4.29}$$

Inequality (4.29) determines slab widths (or path lengths in fractal media) for which the quantity T_0 gives

a good approximation for the exact transmission coefficient. It is interesting to compare it with requirement (3.3) for the Born approximation to be valid. In most cases in principle one can put $A(1 + \epsilon_{\max}) \sim 1$ without loss of generality. Then (4.29) can be rewritten as $kL \leq 1/a_N$. Since we are interested in k being large enough, we have $a_N \ll 1$. Thus the region (4.26) is much larger than (3.3). If the wavelength ($\lambda \sim k^{-1}$) coincides with the scale of the lowest harmonic (i.e., the tone with number $N=0$) the regions coincide with each other.

To conclude this section, note that the region of the TSM applicability is much larger than (4.29) if Eq. (4.21) cannot be satisfied, i.e., if there are not stationary-phase points.

V. SCATTERING DATA OF THE WEIERSTRASS-TYPE PERMITTIVITY

Let us go on to examples and start with the wave transition through a medium with the permittivity described by the Weierstrass function (2.3). In accordance with the discussion we split $\epsilon_N(x)$ in the following way [16]:

$$\epsilon_N(x) = \epsilon_0(1 - \gamma^{D-2}) \sum_{n=0}^{N-1} \frac{\cos(\gamma^n x)}{\gamma^{(2-D)n}} \tag{5.1}$$

and

$$\begin{aligned} \Delta\epsilon_N(x) &= \epsilon_0(1 - \gamma^{D-2}) \sum_{n=N}^{\infty} \frac{\cos(\gamma^n x)}{\gamma^{(2-D)n}} \\ &= \gamma^{(D-2)N} \epsilon_W(\xi), \end{aligned} \tag{5.2}$$

with $\xi = \gamma^N x$.

It is not difficult to give the upper bound for $\Delta\epsilon_N(x)$ using the formula for the geometrical progression:

$$|\Delta\epsilon_N(x)| \leq \gamma^{(D-2)N} \frac{\epsilon_0}{1 - \gamma^{D-2}}. \tag{5.3}$$

Hence requirement (4.3) can be replaced by

$$\gamma^{(2-D)N} \gg 1. \tag{5.4}$$

The estimation of the derivative $\epsilon_N(x)$ with respect to x as a finite geometrical progression yields

$$\left| \frac{d\epsilon_N(x)}{dx} \right| \leq \gamma^N (\gamma^{(D-2)N} - \gamma^{-N}) \frac{1 - \gamma^{D-2}}{\gamma^{D-1} - 1}. \tag{5.5}$$

From the comparison of (5.5) with the requirement (4.4) we get

$$\gamma^{(D-1)N} \ll k. \tag{5.6}$$

At last, in accordance with (4.15), equating $k = \gamma^N$ we find that the TSM is applicable to the Weierstrass function $\epsilon_W(x)$ if

$$k^{2-D} \gg 1 \tag{5.7}$$

and the dividing number is defined by

$$N = \ln k / \ln \gamma. \tag{5.8}$$

Resonance scattering

Considering $T_0(L)$, we find that it possesses a number of characteristic scales. The smallest of them is determined by the cosine in the denominator and describes the mentioned resonance effects: the dependence T_0 versus L has oscillations with the period l_W proportional to the wavelength:

$$l_W \propto 2\pi/k. \tag{5.9}$$

In order to understand the nature of another scale let us consider Fig. 1, where the Weierstrass function is depicted. If we cut off this function by any point L , examine the value $\epsilon_W(L)$ averaged over small oscillations and take into account that $\epsilon_W(L)$ plays the part of a "level" of the second effective boundary in Eq. (4.16), we find that this level changes as the slab width increases. The two most evident scales are designated in Fig. 1 by points A and B . The largest scale is that of the order of the A -point ordinate. The interval (A, B) corresponds to another scale. It is natural to expect that the scattering data reflect such behavior of the permittivity.

To illustrate this we study numerically R_0 bounded with T_0 by the relation

$$R_0 = 1 - T_0 \tag{5.10}$$

as a function of L for different parameters γ and D . Keeping in mind the numerical test of the applicability region of the TSM we present in Figs. 2 and 3 both the direct numerical solution of the Riccati equation and the

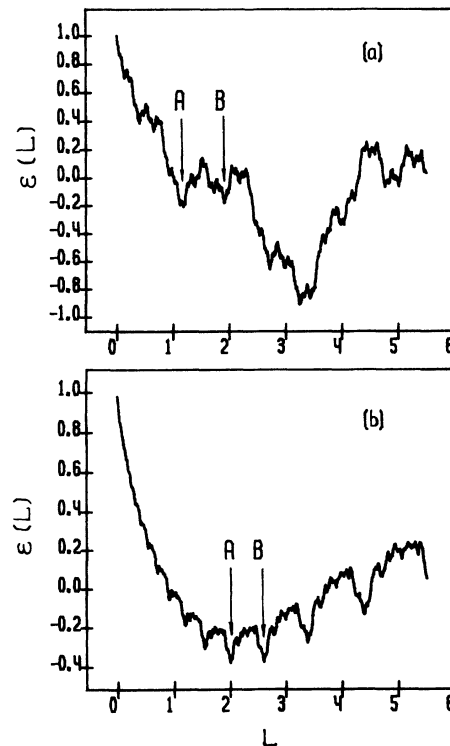


FIG. 1. The Weierstrass function for $D=1.3$, $N=20$, and different parameters γ : (a) $\gamma=2.9$; (b) $\gamma=1.3$.

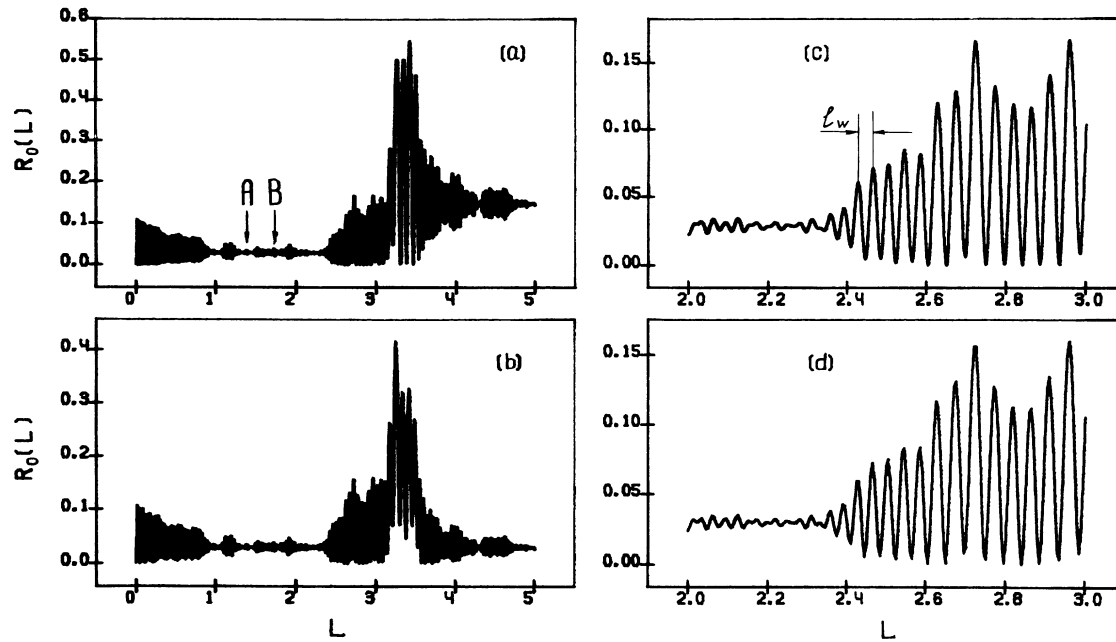


FIG. 2. The reflection coefficient of the Weierstrass-type fractal slab, having parameters $\gamma=2.9$ and $D=1.3$, $\epsilon_0=1$, vs slab width for the incident wave number $k=100$: plots (a) and (c) are the direct numerical solution of the Riccati equation in the different scales. Plots (b) and (d) are the graphical representation of R_0 expressed by (4.15) and (5.10).

calculation of R_0 with the help of the developed method [i.e., according to the formulas (5.10) and (4.16)].

As is seen from comparison of Figs. 2(a), 2(b) and 3(a), 3(b) with the corresponding shape of the Weierstrass function [Figs. 1(a) and 1(b)] there is a good agreement between pairs of scales designated by points A and B. The oscillations of scale l_w [see Eq. (5.9)] are pronounced on Figs. 2(c), 2(d) and 3(c), 3(d).

To support our reasoning, we give some details about the numerical procedure itself. The question of correspondence between computing results obtained by (2.7) and (2.8) and those obtained by the TSM is not evident. The essence of this remark is as follows.

All mismatches between computing and analytical results arise due to either the unavailability of the TSM in some region (say, far from the origin) or digital accuracy

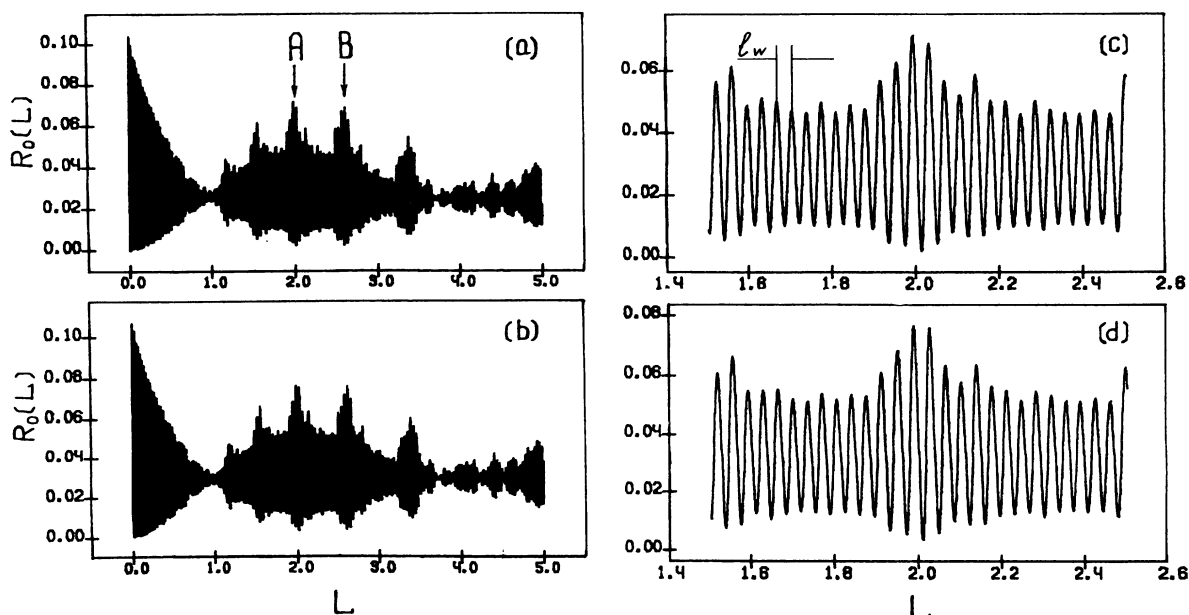


FIG. 3. The same as Fig. 2, but for $\gamma=1.3$.

accompanying every numerical method (where an analytical approach is appropriate).

To integrate the Riccati equation we used the well-known Runge-Kutta method (see, e.g., [26]) with an automatically varying step. This method allows one to avoid the situation when the integration step is equal to or larger than the characteristic scale of a function under calculation. The last notification is not in agreement with the reasoning of Sec. III, where we declared that the fractal structures have all scales. However, this disagreement arises only at first sight. In order to explain this one has to answer the question: is there any “effective” number of harmonics that simultaneously provides (within the framework of the numerical method) all affects discussed above and gives sufficient calculation accuracy. The solution is given by the accuracy test presented in Fig. 4. Here we study the dependence of R on a harmonic number of the band-limited Weierstrass function at $L = \text{const}$. Figure 4 shows that all plots have saturation limits which are true and are achieved at some numbers N_{\min} . For example, for $k = 100$ we have

$$\begin{aligned} N_{\min} &= 5 \quad \text{at } \gamma = 2.9, \\ N_{\min} &= 10 \quad \text{at } \gamma = 2.0, \\ N_{\min} &= 20 \quad \text{at } \gamma = 1.3. \end{aligned} \tag{5.11}$$

Thus N_{\min} grows as γ decreases, which is a consequence of a worse convergence of the Weierstrass set at small γ .

All curves in the present paper are calculated with accuracy providing

$$\frac{\Delta R}{R_0} \ll a_{\min}, \tag{5.12}$$

where ΔR is the corresponding function increment on each Runge-Kutta step and a_{\min} is an amplitude of a tone of number $n = N_{\min}$. The inequality (5.12) yields the rela-

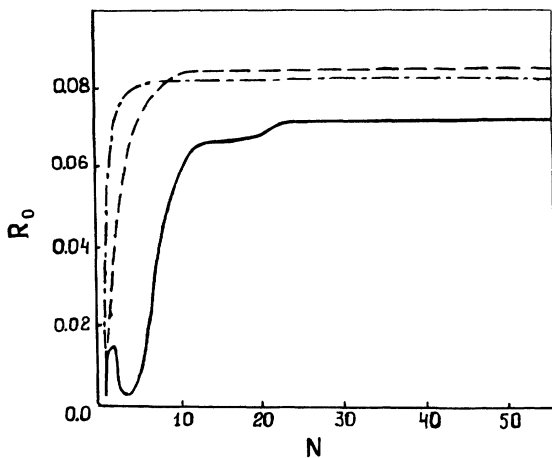


FIG. 4. The dependence of the reflection coefficient R_0 on the number N of harmonics of the Weierstrass function has been taken for calculations for different γ values and slab width $L = 0.1$; solid, dashed, and dot-dashed lines correspond to $\gamma = 1.3$, $\gamma = 2.0$, and $\gamma = 2.9$. All plots are depicted for $D = 1.3$ and $k = 100$. There are three satiate limits.

tion between N_{\min} and a Runge-Kutta step. It should be noted also that the digital accuracy (i.e., the number of digital figures) is supported in a maximum value (32 significant figures for our computer).

The point of the principle is that the results of the accuracy test just obtained could be predicted analytically from the TSM. Indeed, as far as the leading order of the reflection coefficient is determined by the boundary scattering, all harmonics with wave numbers greater than γ^N do not give the contribution (they result in the fractal scattering only). Hence, under the numerical solution of the Riccati equation we can take into account only tones with numbers less than

$$N = N_{\min} = \left\lfloor \frac{\ln k}{\ln \gamma} \right\rfloor + 1 \tag{5.13}$$

[see Eq. (5.7)]. Here the brackets stand for the integer part. Inserting $k = 100$ into this equation one can easily get for $\gamma = 1.3, 2.0, 2.9$ the result (5.11) previously found numerically.

Returning to Figs. 2 and 3 one can see by comparison of plots (a), (b) and (c), (d) the excellent coincidence of the TSM results and those found by direct calculations on distances up to some limits depending on problem parameters. By estimations obtained from our numerical calculations, these limits reach $L \sim 20$ at $k = 100$, $\gamma = 1.3$, and $D = 1.3$ (in order to make the picture observable we restrict it by point $L = 5$) (Fig. 2) and $L \sim 3$ for the same k and D but $\gamma = 2.9$ (Fig. 3). Thus in both cases we have $a_k k L \sim 1-10$. Hence the TSM is applicable in a larger region than that obtained from estimates [see Eq. (4.29)]. The explanation of this fact is simple enough. The TSM fails because of resonant scattering by one of the harmonics from the fractal part of the permittivity $\Delta \epsilon_N(x)$. Harmonic amplitudes decrease according to the exponential law. That is why, if resonant scattering occurs due to a harmonic with number $(N + n')$, the estimation (4.29) may be improved in $\gamma^{n'}$ times.

Finally, we investigated the reflection coefficient R_0 as a function of the box dimension D . The results obtained by the Runge-Kutta method from Eqs. (2.7) and (2.8) and by analytical formulas (4.15) and (5.10) are represented in Fig. 5. One can see a good correspondence between methods discussed up to $D \sim 1.6$. The mismatch for $D \geq 1.6$ and evident nonsense $R(D = 2) = 0$ can be explained in the following way. Let us return to requirement (4.29). In the case under consideration it is equivalent to the restriction for the dimension:

$$D \leq 1 - \frac{\ln L}{\ln k}. \tag{5.14}$$

Substituting $L = 0.1$ and $k = 100$ we obtain $D \leq 1.5$. Hence the TSM fails at $D \rightarrow 2$. It manifests itself in the anomalous fractal scattering (cf. the result of the Born approximation in Sec. III). Moreover, if $D \rightarrow 2$ the normalizing factor in the definition (2.3) goes to zero while the numerical calculation is carried out without changing of the harmonics number. It is a reason for the “non-physical” decreasing of R_0 near the point $D = 2$.

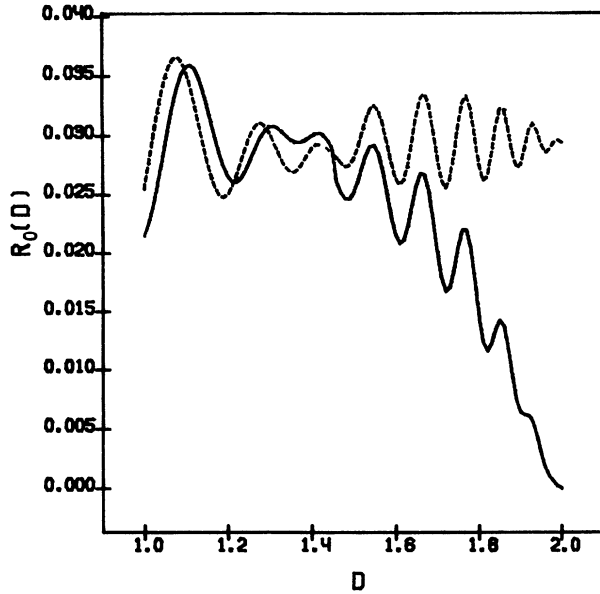


FIG. 5. The reflection coefficient R_0 as a function of the box dimension D for $L=1.0$, $k=100$ and the Weierstrass function with $\gamma=1.3$. The outcomes calculated by the Runge-Kutta method and by the TSM are depicted by solid and dashed lines, respectively.

VI. SCATTERING DATA OF THE SINGULAR PERMITTIVITY

The TSM is inapplicable for calculation of the reflection coefficient of the medium with permittivity (2.4). Indeed, it is impossible to satisfy the requirement (4.3), which follows from the asymptotic behavior (2.5). At the same time, this difficulty is connected with the singular points ($x=2\pi l$, $l=0,1,2,\dots$) of the expansion rather than with the irregular structure. It becomes evident if we study the wave propagation through a slab having the permittivity

$$\epsilon_\alpha^*(x) = \epsilon_\alpha(x + L^*), \quad (6.1)$$

with L^* being a constant less than π ($L^* < \pi$), x varying inside the interval $[0; 2(\pi - L^*)]$ and $\epsilon_\alpha(x)$ determined by (2.4). Then according to the TSM we write

$$\epsilon_N^*(x) = \epsilon_0 \sum_{n=1}^{N-1} \frac{\cos[n(x + L^*)]}{n^\alpha} \quad (6.2)$$

and

$$\Delta\epsilon_N^*(x) = \epsilon_0 \sum_{n=N}^{\infty} \frac{\cos[n(x + L^*)]}{n^\alpha}. \quad (6.3)$$

First, consider the requirement (i) from Sec. IV A. The set $\Delta\epsilon_N^*(x)$ can be evaluated as follows (see Appendix B):

$$|\Delta\epsilon_N^*(x)| < \epsilon_0 \frac{L}{N^\alpha \left| \sin \frac{L^*}{2} \right|}. \quad (6.4)$$

The upper estimation for $|\epsilon_N^*(x)|$ has the form

$$|\epsilon_N^*(x)| \leq \frac{\epsilon_0}{\left| \sin \frac{L^*}{2} \right|}, \quad (6.5)$$

which is a simple consequence of Abel's theorem [18,27]. Hence the condition for the TSM to be applicable takes the form

$$N \gg 1. \quad (6.6)$$

Taking this into account, for the derivative of $\epsilon_N^*(x)$ with respect to x one can use the asymptotic formula [29]

$$\left| \frac{d\epsilon_N^*(x)}{dx} \right| \leq \epsilon_0 C N^{1-\alpha} \text{ at } N \rightarrow \infty, \quad (6.7)$$

where C is a constant.

In accordance with (4.15) one has to put

$$N = k. \quad (6.8)$$

Consequently the requirement (6.6) is a sufficient condition for the smoothness of the truncated permittivity $\epsilon_N^*(x)$.

It is necessary to stress that the comparison of Eqs. (6.4) and (6.5) makes sense only if L^* is not small enough. Indeed, under the condition (6.6) the value of $|\epsilon_N^*(x)|$ allows another upper bound ϵ_{up} which can be estimated as

$$\epsilon_{\text{up}} \sim \epsilon_0 \frac{N^{-\alpha}}{1-\alpha}. \quad (6.9)$$

Hence, for the smallness of $|\Delta\epsilon_N^*(x)|$ at $L^* \rightarrow 0$ one has to require

$$k \gg \frac{(1-\alpha)}{\left| \sin \frac{L^*}{2} \right|}. \quad (6.10)$$

As can be easily shown by comparison of this condition with Eq. (3.8) there is no overlapping between the applicability regions of the TSM and the Born approximation at any L^* . This means that for $L^* \rightarrow 0$ the first one cannot be used.

The Born scattering discussed in Sec. III does not exhaust all peculiarities of the permittivity under consideration. Indeed, there is such a quantity α_0 that the corresponding partial sums $\epsilon^*(x) = \epsilon_N^*(-L^*)$, $N=1,2,\dots$ have a homogeneous interior limit at $\alpha > \alpha_0$ and do not have it at $\alpha < \alpha_0$ [18]. The value α_0 approximately equals 0.15. This means that we cannot introduce a normalization to make $1 + \epsilon_N^*(x) > 0$ at any x and given N , i.e., to exclude the turning points in the Helmholtz equation with a cutoff potential (4.6). Hence, corresponding outcomes will have no physical meaning and will not display any real processes unless the TSM is specially modified for such a case. Hence in order to present the scattering data in the form (4.13) one has to assume

$$\alpha > \alpha_0 \quad (6.11)$$

and has to make sure that the interior boundary of $\epsilon_N^*(x)$ is larger than -1 .

The discussed effect is especially important for the nu-

merical investigation of the problem. Indeed, since any numerical scheme deals only with a truncated sum, only the results obtained under condition (6.11) can be satisfactorily interpreted. This situation seems to be typical for fractal problems: there are delicate fractal effects which cannot be observed in a direct numerical experiment because of the importance of spectrum tails (or far series items) for such phenomena.

We investigate numerically only the case $\alpha > \alpha_0$. Otherwise, when $\alpha < \alpha_0$, all numerical schemes are divergent.

Returning to the TSM we note that in its turn the interval $(\alpha_0; 1)$ has to be divided into two subintervals. The first of them close to α_0 is that of anomalous scattering. Here the TSM is unsuitable due to reasons that have been discussed in Sec. V. It is clearly demonstrated in Fig. 6. It should be noted that characteristic scales and approximate positions of the "reflection coefficient flashes" are similar for data obtained by the TSM and by numerical

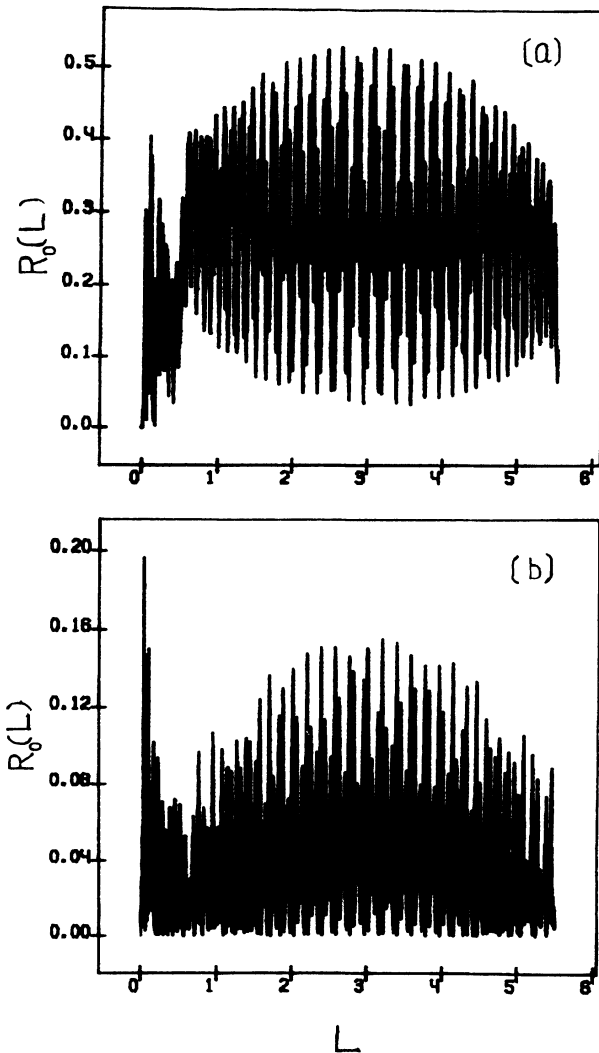


FIG. 6. The reflection coefficient of the singular permittivity as a function on the slab width obtained from the Riccati equation (a) and within the framework of the TSM (b) for $\alpha=0.3$ and $k=100$; $L^*=0.1$.

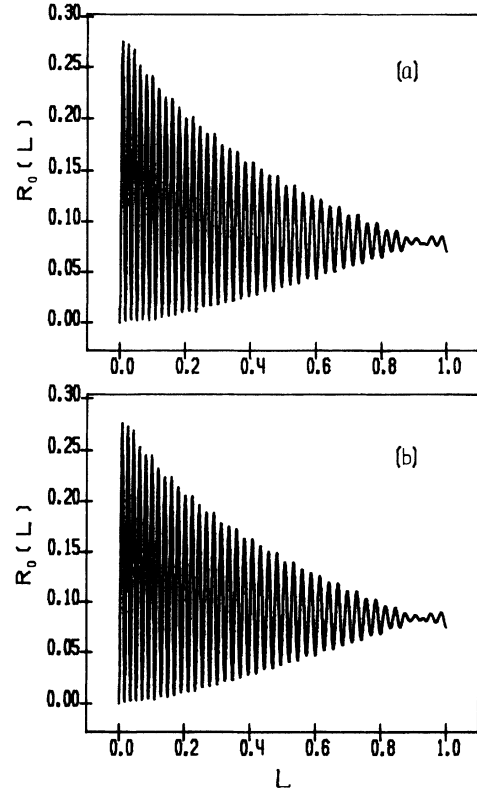


FIG. 7. The same as in Fig. 6, but for $\alpha=0.95$.

calculations.

The region near $\alpha=1$ (see Fig. 7) can be described well by the TSM. To specify this region now we obtain the dividing point α^* . To this end we insert the estimation (6.5) and relation $a_k \sim k^{-\alpha}$ into the requirement (4.29). Then the latter can be represented as follows:

$$\alpha > \alpha^* = \frac{1 - \ln[|\sin(L^*/2)|/L\epsilon_0]}{\ln k} \quad (6.12)$$

The nature of this phenomena is similar to that discussed in the case of the Weierstrass function [see Eq. (5.14)]. Really this estimation is sufficiently rough so that α^* in the experiment is less than that just obtained. It is demonstrated by the numerical investigation of the reflection coefficient of a slab with the permittivity $\epsilon_\alpha^*(x)$. As for the Weierstrass function one can see an excellent coincidence of the results in both plots 7(a) and 7(b) calculated with the help of the Riccati equation and representation (4.16). Such a coincidence we observed up to $L \sim 3.5$, which corresponds to $[1 + \epsilon_\alpha^*(x)]a_k kL \sim 80$, i.e., to exceeding of the accuracy predicted in (4.29) [or (6.13)].

VII. CONCLUSION

We have considered the scattering data of fractal layers of restricted widths. Briefly the results can be summarized as follows. The fractal scattering has a "singular" character. It becomes observable in the Born approxima-

tion and manifests itself in the anomalous amplifying of scattering by the small-scale structure: the reflection coefficient of a fractal slab grows with the slab width, increasing according to a “noninteger” power law.

In spite of the fact that the WKB approximation in the usual sense is not applicable to diffractal problems, it is possible to develop the two-scale technique. This technique allows one to determine a region where the WKB approximation can be applied to truncated permittivity. The small scale scattering in this case gives a small contribution to the scattering data in comparison with the boundary scattering. That is why resonance effects determine the behavior of diffractals. At the same time in the problem under consideration the resonance scattering has some peculiarities in comparison with conventional resonance effects. The most important of them is that the level of a second effective boundary depends on the wave number and slab width. It allows one to believe that investigation of the transmission (reflection) coefficient versus wave number in the respective region could give information on an envelope of a fractal-medium permittivity with high accuracy (cf. Figs. 1, 2, and 3). Moreover, a branch of less wavelengths will give an envelope of less scales. Meantime, a local (to all appearance, box) dimension of a scattering structure is determined by the small-scale scattering. The digital consideration of the corresponding contribution to the scattering data deviates from the theme of the present work.

However, the TSM fails in the case of singular permittivity. In order to study such systems one has to take into account that any point singularity has a mathematical character rather than physical one. Thus, to regularize the problem, it is necessary to restrict all functions in accordance with the physical statement. After this, the TSM is valid.

In connection with this it should be pointed out that any real physical medium can be a fractal only in a limited region of scales. Hence the question of great importance is that of correspondence between the mathematics of the TSM and real fractal structures having a finite range of scales. There is an evident answer. If l is the smallest value (as above L is the largest one) and requirement (4.26) is satisfied, the TSM has a meaning at $l \ll k^{-1} \ll L$. The band limited small-scale structure will give only corrections for the “fractal” part of the transmission coefficient, which is small as long as L is not very large.

In the Introduction we have pointed out the paper by Jaggard and Sun [12]. They observed that the diffractal “insensitivity to the number of tones N used in the Weierstrass corrugation function if N is sufficiently large.” Our analytical and numerical results show the same behavior. Moreover, we can state that this is a common property of a wide class of fractal-scattering problems. The accuracy of numerical simulations must be of sufficient order to take into account all tones of scales greater than the wavelength. Further increasing of the accuracy by means of including more and more harmonics will give small corrections if boundary scattering is essential.

The TSM can be easily generalized for the description of functions given in a form of their spectrum (namely,

for such functions the TSM has been used in the theory of surface scattering [23,24]). As is evident, truncating the Fourier series can be provided by the simple averaging over a spatial region of wavelength scale order. Corresponding results will be presented elsewhere.

ACKNOWLEDGMENTS

We are thankful to Professor F. G. Bass for stimulating discussions and Professor I. M. Fuks for a number of useful comments. We also wish to thank Professor D. L. Jaggard for having sent reprints of his papers. V.V.K. is grateful to Professor J. Llosa for remarks that promoted a more accurate statement of the problem.

APPENDIX A

Note that Eq. (3.2) under the condition (2.3) can be rewritten in the form

$$R = -\frac{k\epsilon_0}{2}(1-\gamma^{D-2}) \sum_{n=0}^{\infty} \frac{f(\gamma^n L; L)}{\gamma^{(2-D)n}(4k^2-\gamma^{2n})}, \tag{A1}$$

where

$$f(x; L) = 2k(\cos x - 1) + \frac{i}{2L} x \sin x. \tag{A2}$$

Following Hughes, Montroll, and Shlesinger [28] we introduce the inverse Mellin transform:

$$f(x, L) = \frac{1}{2\pi i} \int_{C-i\infty}^{C+i\infty} x^{-p} F(p; L) dp. \tag{A3}$$

In the case (A2) we have

$$F(p; L) = 2k \Gamma(p) \cos \left[\frac{\pi p}{2} \right] + \frac{i}{L} \Gamma(p+1) \sin \left[\frac{\pi}{2}(p+1) \right], \tag{A4}$$

with $-1 < p < 0$.

Combining (A3) with (A1) one can present the reflection coefficient in the form

$$R = -\frac{k\epsilon_0}{4\pi i} (1-\gamma^{D-2}) \int_{C-i\infty}^{C+i\infty} dp L^{-p} F(p; L) \times \sum_{n=0}^{\infty} \frac{\gamma^{(2-D+p)n}}{4k^2-\gamma^{2n}}. \tag{A5}$$

If the wave vector is not very large, i.e.,

$$k < \frac{1}{2},$$

simple algebra allows one to rewrite the sum in the right-hand side of Eq. (A5) as

$$-\sum_{m=0}^{\infty} (2k)^{2m} \frac{1}{1-\gamma^{-[p-D+2(m+2)]}}$$

and correspondingly

$$R = \frac{k\epsilon_0}{4\pi i} (1-\gamma^{D-2}) \sum_{m=0}^{\infty} (2k)^{2m} \int_{C-i\infty}^{C+i\infty} dp (1-\gamma^{-[\rho-D+2(m+1)]})^{-1} L^{-\rho} F(\rho, L). \tag{A6}$$

The advantage of the latter representation consists of the expansion of the reflection coefficient into the power series of the wave vector in the evident form. Inserting (A4) into (A6) we come to the necessity to calculate integrals

$$J_{C,m} = \int_{C-i\infty}^{C+i\infty} dp \frac{L^{-\rho} \Gamma(\rho) \cos\left[\frac{\pi p}{2}\right]}{1-\gamma^{-[\rho-D+2(m+2)]}}$$

and

$$J_{S,m} = \int_{C_1-i\infty}^{C_1+i\infty} dp \frac{L^{-\rho} \Gamma(\rho+1) \cos\left[\frac{\pi p}{2}\right]}{1-\gamma^{-[\rho-D+2(m+2)]}}.$$

Let us consider the first integral. It has two series of simple poles. The first one is produced by the Γ function and consists of all negative integers. The second set is raised by the denominator and consists of points

$$p_n = \frac{2\pi i n}{\ln \gamma} - 2(m+2) + D. \tag{A7}$$

It is evident that the value $J_{C,m}$ can be considered as the limiting transition ($M \rightarrow \infty$) of the corresponding integral between points $C-iM$ and $C+iM$. Thus, evaluating the integral around the contour that bounds points $C \pm iM$ and $C_1 \pm iM$ [where $-1 < C < 0$; and $-2(m+3) < C_1 < -2(m+2)+1$] with the help of the residue theory and making the mentioned limiting transition we obtain

$$J_{C,m} = \frac{2\pi i}{D-2(m+2)\ln \gamma} \sum_{n=-\infty}^{\infty} \Gamma(p_n) \cos\left[\frac{\pi p_n}{2}\right] \exp(-p_n \ln L) + 2\pi i \sum_{n=1}^{m+2} \frac{(-1)^n L^{2n}}{(2n)!(1-\gamma^{-[2n+D-2(m+2)])}} + \int_{C_1-i\infty}^{C_1+i\infty} dp \frac{L^{-\rho} \Gamma(\rho) \cos\left[\frac{\pi p}{2}\right]}{1-\gamma^{-[\rho-D+2(m+2)]}}. \tag{A8}$$

By analogy, for $J_{S,m}$ we have

$$J_{S,m} = \frac{2\pi i}{D-2(m+2)\ln \gamma} \sum_{n=-\infty}^{\infty} p_n \Gamma(p_n) \cos\left[\frac{\pi p_n}{2}\right] \exp(-p_n \ln L) + 2\pi i \sum_{n=1}^{m+2} \frac{(-1)^{n+1} L^{2n}}{(2n)!(1-\gamma^{-[2n+D+2(m+2)])}} + \int_{C_1-i\infty}^{C_1+i\infty} dp \frac{L^{-\rho} \Gamma(\rho+1) \cos\left[\frac{\pi p}{2}\right]}{1-\gamma^{-[\rho-D+2(m+2)]}}. \tag{A9}$$

Inserting expressions (A8) and (A9) into (A6) and leaving only the terms of the lowest order with respect to L we get the result (3.4). Note that the main contribution is given by the first terms in the both series in the right-hand side of Eq. (A9).

APPENDIX B

It is evident that the series (6.3) can be rewritten in the form

$$\Delta \epsilon^*(x) = \epsilon_0 \cos[N(x+L^*)] \sum_{m=0}^{\infty} \frac{\cos[m(x+L^*)]}{(m+N)^\alpha} - \epsilon_0 \sin[N(x+L^*)] \sum_{m=0}^{\infty} \frac{\sin[m(x+L^*)]}{(m+N)^\alpha}. \tag{B1}$$

Let us consider the first sum in the right-hand side of this presentation. There is the following sequence of inequalities:

$$\left| \sum_{m=0}^{\infty} \frac{\cos(mx)}{(m+N)^\alpha} \right| \leq \frac{1}{N^\alpha} + \left| \sum_{m=1}^{\infty} \frac{\cos(mx)}{(m+N)^\alpha} \right| \leq \frac{1}{N^\alpha} + \frac{1}{(1+N)^\alpha \left| \sin \frac{x}{2} \right|} \leq \frac{1}{N^\alpha} \left[1 + \frac{1}{\left| \sin \frac{x}{2} \right|} \right] \leq \frac{2}{N^\alpha \left| \sin \frac{x}{2} \right|}. \tag{B2}$$

The relation between the second and third items of this sequence is provided by Abel's theorem [18,27]. The same estimate is valid for the second integral in the right-hand side of Eq. (B1). Thus trivial algebra gives (6.4).

*Present address: Departamento de Física Teórica I, Facultad de Ciencias Físicas, Universidad Complutense, E-28040 Madrid, Spain.

- [1] B. B. Mandelbrot, *The Fractal Geometry of Nature* (Freeman, New York, 1982).
- [2] J. Feder, *Fractals* (Plenum, New York, 1988).
- [3] M. V. Berry, *J. Phys. A* **12**, 781 (1979).
- [4] A. Le Mehaute and F. Heliodore (unpublished); F. Heliodore and A. Le Mehaute (unpublished).
- [5] M. V. Berry and T. M. Blackwell, *J. Phys. A* **14**, 3101 (1981).
- [6] Po-zen. Wong and A. J. Bray, *Phys. Rev. B* **32**, 7417 (1985).
- [7] E. Jakeman, in *Fractals in Physics*, edited by L. Pietronero and E. Tosatti (North-Holland, Amsterdam, 1986).
- [8] D. L. Jaggard and Y. Kim, *J. Opt. Soc. Am.* **4**, 1055 (1987).
- [9] Po-zen. Wong, *Phys. Rev. B* **32**, 7417 (1985).
- [10] S. K. Sinha, E. B. Sirota, S. Garoff, and H. B. Stanley, *Phys. Rev. B* **38**, 2297 (1988).
- [11] D. L. Jaggard and X. Sun, *J. Opt. Soc. Am.* **7**, 1131 (1990).
- [12] D. L. Jaggard and X. Sun, *IEEE Trans. AP-37*, 1591 (1989).
- [13] T. Tel, *Z. Naturforsch. A* **43**, 1154 (1988).
- [14] Jaggard and Sun in their paper [11] have introduced a dimension for band-limited fractals. Such a dimension differs from the box one of corresponding "complete" fractals. From the mathematical point of view a band-limited fractal is a "well-differentiable" function and has the integer topological dimension (it is equal to unity) since it is a finite sum of cosines. It means that such a value may have only any physical treatment rather than a real mathematical one. The projected fractal dimension in the problem of pulse propagation through a fractal slab described by the band-limited Weierstrass function has been introduced by D. L. Jaggard, Y. Kim, and N. Cho [*J. Appl. Phys.* (to be published)]. This kind of dimension is correlated with the box dimension and may serve as a roughness criterion.
- [15] V. V. Konotop, O. I. Yordanov, and I. V. Yurkevich, *Europhys. Lett.* **12**, 481 (1990).
- [16] V. V. Konotop, *Phys. Rev. A* **44**, 1352 (1991).
- [17] M. V. Berry and Z. V. Lewis, *Proc. R. Soc. London Ser. A* **370**, 459 (1980).
- [18] A. Zigmund, *Trigonometric Series* (Cambridge University Press, Cambridge, England, 1959), Vol. 1.
- [19] I. M. Lifshits, S. A. Gredeskul, and L. A. Pastur, *Introduction to the Theory of Disordered Systems* (Nauka, Moscow, 1976).
- [20] *Handbook of Mathematical Functions*, Natl. Bur. Stand. Appl. Math. Ser. No. 55, edited by M. Abramowitz and I. A. Stegun (U.S. GPO, Washington, DC, 1964).
- [21] N. Froman and P. O. Froman, *JWKB Approximation* (North-Holland, Amsterdam, 1965).
- [22] M. V. Fedor'uk, *Asymptotic Methods for Linear Differential Equations* (Nauka, Moscow, 1983) (in Russian).
- [23] B. F. Kur'yanov, *Akust. Z.* **8**, 305 (1962) (in Russian).
- [24] Yu. A. Lementa and I. M. Fuks, *Izv. Vyssh. Uchebn. Zaved. Radiofiz.* **21**, 379 (1978).
- [25] A. Messiah, *Quantum Mechanics* (Wiley, New York, 1961).
- [26] J. C. Butcher, *Lect. Notes Math.* **109**, 133 (1969).
- [27] N. K. Bari, *Trigonometric Sets* (Moscow, Fizmatgiz, 1961) (in Russian).
- [28] B. D. Hughes, E. W. Montroll, and M. F. Schlesinger, *J. Stat. Phys.* **28**, 111 (1982).
- [29] It is a consequence of the asymptotic formula $\sum_{n=1}^N n^\gamma \sin nx = O(N^\gamma)$ at $N \rightarrow \infty$. See, e.g., M. V. Fedor'yuk, *Asymptotic Integrals and Series* (Moscow, Nauka, 1987).